The Repertoire of Newly Developing Regulatory T Cells in the Type 1 Diabetes–Prone NOD Mouse Is Very Diverse

Ariel Galindo-Albarrán, Sarah Castan, Jérémy C Santamaria, Olivier P Joffre, Bart Haegeman, Paola Romagnoli, Joost P M van Meerwijk

▶ **To cite this version:**

Ariel Galindo-Albarrán, Sarah Castan, Jérémy C Santamaria, Olivier P Joffre, Bart Haegeman, et al.. The Repertoire of Newly Developing Regulatory T Cells in the Type 1 Diabetes–Prone NOD Mouse Is Very Diverse. Diabetes, 2021, 70 (8), pp.1729 - 1737. 10.2337/db20-1072 . inserm-04670670

HAL Id: inserm-04670670

https://inserm.hal.science/inserm-04670670v1

Submitted on 12 Aug 2024

HAL is a multi-disciplinary open access archive for the deposit and dissemination of scientific research documents, whether they are published or not. The documents may come from teaching and research institutions in France or abroad, or from public or private research centers.

L'archive ouverte pluridisciplinaire **HAL**, est destinée au dépôt et à la diffusion de documents scientifiques de niveau recherche, publiés ou non, émanant des établissements d'enseignement et de recherche français ou étrangers, des laboratoires publics ou privés.

Distributed under a Creative Commons Attribution - NonCommercial - NoDerivatives 4.0 International License

Check for updates

The Repertoire of Newly Developing Regulatory T Cells in the Type 1 Diabetes–Prone NOD Mouse Is Very Diverse

Ariel Galindo-Albarrán,[1,2] Sarah Castan,[1] Jérémy C. Santamaria,[1] Olivier P. Joffre,[1] Bart Haegeman,[2] Paola Romagnoli,[1] and Joost P.M. van Meerwijk[1]

Diabetes 2021;70:1729–1737 | https://doi.org/10.2337/db20-1072

Regulatory T lymphocytes expressing the forkhead/winged helix transcription factor Foxp3 (Treg) play a vital role in the protection of the organism from autoimmune disease and other immunopathologies. The antigen specificity of Treg plays an important role in their in vivo activity. We therefore assessed the diversity of the T-cell receptors (TCRs) for antigen expressed by Treg newly developed in the thymus of autoimmune type 1 diabetes-prone NOD mice and compared it to the control mouse strain C57BL/6. Our results demonstrate that use of the TCRα and TCRβ variable (V) and joining (J) segments, length of the complementarity determining region (CDR) 3, and the diversity of the TCRα and TCRβ chains are comparable between NOD and C57BL/6 mice. Genetic defects affecting the diversity of the TCR expressed by newly developed Treg therefore do not appear to be involved in the etiology of type 1 diabetes in the NOD mouse.

Regulatory T lymphocytes expressing the forkhead/winged helix transcription factor Foxp3 (Treg) play a major and even vital role in the control of innate and adaptive immunity and are also involved in tissue repair (1–3). Using a large variety of suppressor-effector mechanisms, Treg inhibit immunity and thus avoid autoimmune pathology, chronic inflammation, and rejection of the semiallogeneic fetus (2). The vital character of immune regulation by Treg is best illustrated by the rapidly lethal autoimmune and inflammatory syndromes that develop in humans and mice carrying loss-of-function mutations in the locus encoding the master regulator of Treg development and function, FOXP3/Foxp3 (4,5). More subtle defects in Treg may be involved in the etiology of autoimmune pathology (6).

Treg can differentiate from T-cell precursors during T-cell development in the thymus and from mature conventional T lymphocytes during immune responses in the periphery (2). In the thymus, Treg development requires high affinity interactions of the T-cell receptor (TCR) for antigen expressed by T-cell precursors with MHC/peptide complexes expressed mainly by medullary thymic stromal cells (7). Because the latter cells present peptides derived from tissue antigens, in part through the action of the transcription factor autoimmune regulator (AIRE) (8), an autospecific Treg repertoire thus develops (9,10). Treg development in the thymus also requires cytokines, such as interleukin-2 (IL-2) and IL-15 (11), as well as signals through costimulatory receptors (12–14).

Defects in Treg development are thought to be involved in the etiology of autoimmune pathology (6). Thus, the very aggressive and rapidly lethal autoimmune syndrome developing in AIRE-deficient NOD mice appears, at least in part, due to defective selection of the Treg repertoire early in life (15). Also mice deficient in IL-2 or its receptor rapidly succumb to autoimmune pathology, but the respective roles of defective intrathymic development and peripheral survival and function of Treg remain to be assessed (11). NOD mice deficient in CD28, in which substantially fewer Treg develop in the thymus, also develop more aggressive type 1 diabetes (T1D) (16).

It has been suggested that the TCR repertoire expressed by Treg developing in the thymus of T1D-prone NOD

[1]Toulouse Institute for Infectious and Inflammatory Diseases (Infinity), INSERM UMR1291–CNRS UMR5051–Université Paul Sabatier (UPS), Toulouse, France
[2]Station d'Écologie Théorique et Expérimentale, CNRS–Université Paul Sabatier (UPS), Moulis, France

Corresponding author: Joost P.M. van Meerwijk, joost.van-meerwijk@inserm.fr

Received 28 October 2020 and accepted 17 May 2021

This article contains supplementary material online at https://doi.org/10.2337/figshare.14611911.

© 2021 by the American Diabetes Association. Readers may use this article as long as the work is properly cited, the use is educational and not for profit, and the work is not altered. More information is available at https://www.diabetesjournals.org/content/license.

mice is less diverse than that developing in the thymus of C57BL/6 (B6) mice, which are frequently used as a T1D-resistant reference (17–19). The results were based on analysis of CD25-expressing $CD4^+CD8^-$ thymocytes, presumably developing Treg. However, our laboratory recently demonstrated that in adult mice, actually only a fraction of thymic Treg are cells that had recently developed, the rest being cells that had recirculated from the periphery back to the thymus (20). Moreover, we recently demonstrated that the NOD thymus contains a particularly high proportion of recirculating Treg (21). Also, CD25 is not only expressed by Treg but also by immature precursors (22). To assess the potential involvement, in the etiology of T1D in the NOD mouse, of genetic defects affecting the diversity of the TCR expressed by newly developed Treg, we therefore readdressed this issue using mutant NOD and B6 mice in which newly developed Treg can be distinguished from recirculating cells and in which Treg can be isolated based on Foxp3 expression.

In *Rag2-Gfp* mice, the *Rag2* promoter drives expression of green fluorescent protein (GFP) (23). Transcription of the GFP encoding sequence thus terminates at positive selection at the CD4/CD8 double-positive stage of T-cell development, and the accumulated GFP degrades with a half-life of 56 h (24,25). In the thymus, newly developed Treg retain sufficient green fluorescence to distinguish them from recirculating cells that had entirely lost fluorescence (20). In *Foxp3-Thy1^a* mice, the allelic cell-surface reporter Thy1.1 is expressed under control of the *Foxp3* promoter, allowing detection of Foxp3-expressing Treg without fixation/permeabilization procedures, thus allowing for isolation of mRNA required for TCR repertoire analysis by high-throughput mRNA sequencing. Using *Rag2-Gfp Foxp3-Thy1^a* mice, we here firmly demonstrate that the TCR repertoire expressed by Treg newly developed in the thymus of the T1D-prone NOD mouse is as diverse as that developing in the resistant mouse strain B6.

RESEARCH DESIGN AND METHODS

Mice

B6 mice expressing the *Foxp3-Thy1^a* mutation and a *Rag2-Gfp* transgene were previously described (26). The two mutations were introduced into the NOD genetic background by speed-backcrossing (27). After all *Idd*-loci were of the NOD allotype (6 generations), the mice were crossed to NOD mice for another 10 generations. Wild-type (WT) NOD.CD45.2 and B6.CD45.1 congenic mice were bred in our colony.

Flow Cytometry

Thymocytes from female 8-week-old WT NOD and B6 mice were incubated with anti-FcRIII/FcRII antibody (2.4G2) and then labeled with EF450-labeled anti-CD8β (H35-17.2), phycoerythrin (PE)-labeled anti-CCR7 (4B12; both from eBioscience), allophycocyanin-Cy7–labeled anti-CD4 (GK1.5), PE-Cy7–labeled CD25 (PC61; both from BD Biosciences), and BV605-labeled anti-CD73 (TY/11.8, Biolegend). The labeled cells were stained with a TCR-Vβ screening FITC-labeled antibody panel (BD Biosciences). Cells were then stained with EF660-labeled anti-Foxp3 (FJK-16s; eBioscience) according to the manufacturer's instructions. The labeled cells were analyzed using a Fortessa flow cytometer (BD Biosciences), and data were analyzed using FlowJo software (Tree Star).

TCR Sequencing

Pooled thymocytes from 8-week-old female *Foxp3-Thy1^a Rag2-Gfp* NOD and B6 mice (n = 8-10) were complement depleted of $CD8^+$ cells using an anti-CD8α hybridoma (31M) supernatant. Remaining cells were stained with PE-labeled anti-CD4 (GK1.5), EF450-labeled anti-CD8β (H35-17.2; both from eBioscience), and allophycocyanin-labeled anti-Thy1.1 (OX7; BD Biosciences). $CD4^+CD8^-Thy1.1^+GFP^+$ Treg ($n = 10^5$) were sorted using the FACSAria II cell sorter (BD Biosciences). TCR sequencing (TCRseq) was performed as previously described, with minor modifications (28,29). mRNA was extracted by NucleoSpin RNA XS (Macherey-Nagel) according to the manufacturer's instructions and was quality controlled (RNA integrity number >8) using the Agilent 2100 BioAnalyzer.

cDNA was prepared as follows: mRNA was reverse transcribed using primers aligning to the sequences encoding the constant regions of TCRα (CTCAGCGTCATGAGCAGGTTAAAT; CAGGAGGATTCGGAGTCCCATAA; TTTTACAACATTCTCCAAGA; TTCTGAATCACCTTTAATGA; ATGAGATAATTTCTACACCT; TTTGGCTTGAAGAAGGAGCG; TTCAAAGCTTTTCTCAGTCA; and TGGTCTCTTTGAAGATATCT) and TCRβ (GGTAGCCTTTTGTTTGTTTG; CCCCTGGCCAAGCACACGAG; TGCCATTCACCCACCAGCTC; GCTATAATTGCTCTCCTTGT; TTGCGAGGATTGTGCCAGAA; CTTGTCCTCCTCTGAAAGCC; and GCCTCTGCACTGATGTTCTG). Then, 5' adapters containing unique molecular identifiers (UMI) were added using a template-switch reaction (TACACGACGCTCTTCCGATCUNNNNUNNNNUNNNNUCTTrGrGrGrG).

Libraries were prepared as follows: The first PCR reaction was performed with 5' primer TACACGACGCTCTTCCGATC and 3' primers AAGTCGGTGAACAGGCAGAG for *Tcra* and TGATGGCTCAAACAAGGAGACC for *Tcrb* (2 min at 95°C, 10 cycles of 20 s at 95°C, 15 s at 59°C, and 45 s at 70°C, and final incubation for 3.5 min at 70°C). The amplicons were then purified using Agencourt AMPure XP beads. The second seminested PCR was performed with 5' primer TACACGACGCTCTTCCGATC and 3' primers AGCAGGTTCTGGGTTCTGGA for *Tcra* and GGGTGGAGTCACATTTCTCAGAT for *Tcrb* (2 min at 95°C, 20 cycles of 20 s at 95°C, 15 s at 59°C, and 45 s at 70°C, and final incubation of 3.5 min at 70°C). The third PCR was performed using 5' primer AATGATACGGCGACCACCGAGATCTACACTCTTTCCCTACACGACGCTCTTCCGATC and 3' primers CAAGCAGAAGACGGCATACGAGAT-

XXXXXXXXGTGACTGGAGTTCAGACGTGTGCTCTTCCGATC-TAGCAGGTTCTGGGTTCTGGA for *Tcra* and CAAGCAGAA-GACGGCATACGAGATXXXXXXXXGTGACTGGAGTTCAGAC-GTGTGCTC TTCCGATCTGGGTGGAGTCACATTTCTCAGAT for *Tcrb* (in which XXXXXXXX is a sequencing index) (2 min at 95°C; one cycle of 20 s at 95°C, 15 s at 59°C, and 45 s at 70°C; five cycles of 20 s at 95°C, 15 s at 75°C, and 45 s at 70°C; and a final incubation of 3.5 min at 70°C). For the fourth PCR, the 5' primer AATGATACGGCGACCACCGA and 3' primer CAAGCAGAAGACGGCATACGA were used (2 min at 95°C; five cycles of 20 s at 95°C, 15 s at 60°C, and 45 s at 70°C; and a final incubation of 3.5 min at 70°C). The quality of each library was verified using the Agilent 2100 BioAnalyzer (mean peak size 640 base pairs). The samples were indexed and sequenced with 300 base pairs paired-end on a MiSeq sequencer (Illumina). Thus, three *Tcra* and three *Tcrb* libraries per mouse strain were generated.

Processing of TCRseq data

The reads were preprocessed with the toolkit pRESTO (30) as follows: FilterSeq was used to select reads with a quality >20. The sequences corresponding to the TCRα constant region (AGCAGGTTCTGGGTTCTGGA) or TCRβ constant region (GGGTGGAGTCACATTTCTCAGAT) and indicating location of the UMI (CTTGGGGG) were searched for using MaskPrimers and PairSeq algorithms and indexed to the head of the paired reads. BuildConsensus was used to construct consensus-sequences of the reads with the same UMI. Next, the forward and reverse reads were aligned to assemble the *Tcra* and the *Tcrb* sequences (AssemblePairs), and the UMI groups containing at least two reads were selected. The sequenced fragments from each selected UMI were aligned to the *Tcra* or *Tcrb* genomic region using the toolkit MiXCR (31) with the tools "align" and "assemble." The aligned fragments were exported as "clonotype-tables" using the tool exportClones.

VDJtools (32) and customized R scripts were used to process these clonotype tables, and graphs were generated. The V-J use plots were generated using the PlotFancyVJUsage command. The CDR3 lengths were calculated based on the information in the clonotype table. The numbers of "P" and "N" nucleotides were extracted from the clonotype tables using the command exportClones VGeneWithP. Rarefaction plots and diversity statistics were calculated and graphed using the R package iNEXTm. We used three different diversity measures: Chao1 estimate, Shannon diversity, and Simpson diversity. All three provide an estimate of the number of clonotypes in the repertoire but differ in the extent to which they discount rare clonotypes. The more rare and therefore difficult to detect clonotypes are discounted, the more precisely the diversity measure can be estimated. By jointly considering these three diversity measures, we cover the full diversity information contained in the sample data (33). All custom scripts used are available at https://github.com/arielgalindoalbarran/NOD_TCR_repertoire.git.

Data and Resource Availability

TCRseq data generated during the current study are available in the Gene Expression Omnibus database (https://www.ncbi.nlm.nih.gov/gds) under accession number GSE1-59001. The other data sets are available from the corresponding author upon reasonable request. The mutant mice used in the current study are available from the corresponding author upon reasonable request.

RESULTS

Only a Limited Proportion of Treg in the Thymus of Adult NOD Mice Are Newly Developed Cells

We and others previously showed that the pool of Treg in the thymus is constituted of newly developed and of fully mature cells. The latter Treg are mostly cells that had recirculated from the periphery back to the thymus. We therefore analyzed NOD mice carrying a *Rag2-Gfp* transgene and the *Foxp3-Thy1*^{a} mutation in which we distinguished newly developed GFP$^+$ from recirculating GFP$^-$, surface Thy1.1$^+$ Treg (20). Using flow cytometry, we found that 32 ± 11% of thymic CD4$^+$CD8$^-$Foxp3$^+$ Treg were GFP$^+$ in 8-week-old NOD females (Fig. 1*A*). This extends our previous finding that in the thymus of adult B6 mice, only a minority of Treg are newly developed cells (20,21). In this study we focused our attention on these newly developed Treg.

V and J Segment Use in TCRα and TCRβ Chains Expressed by Newly Developed NOD and B6 Treg Is Very Similar and Comparably Diverse

To assess the diversity of TCR expressed by newly developed Treg, we first analyzed their TRBV (i.e., TCR-Vβ) repertoire by flow cytometry. The commercially available anti–TCR-Vβ antibody panels are FITC labeled, which is incompatible with the GFP-based identification of newly developed Treg in *Rag2-Gfp* transgenic mice. We therefore identified newly developed nuclear Foxp3$^+$ Treg in WT mice using their CCR7^{high}CD73$^{-/low}$ phenotype that we recently described (21) (Supplementary Fig. 1). Using antibodies to 15 distinct TRBV, we found that the TRBV repertoires expressed by newly developed NOD and B6 Treg were distinct (Supplementary Fig. 2*A*), but similarly diverse, even if the very small difference in the diversities (3.5%) was statistically significant (Fig. 1*B*).

To study the TRAV repertoire expressed by newly developed Treg, we sorted CD4$^+$CD8$^-$Thy1.1$^+$GFP$^+$ thymocytes from *Foxp3-Thy1*^{a} *Rag2-Gfp* NOD and B6 mice, isolated mRNA, and then performed high-throughput TCRseq of *Tcra* mRNA. We used unique UMIs to identify sequences derived from individual mRNAs. Whereas we observed substantial differences between the TRAV-repertoires of NOD and B6 Treg, they were similarly diverse (Fig. 2*A* and Supplementary Table 1). Using TCRseq, we

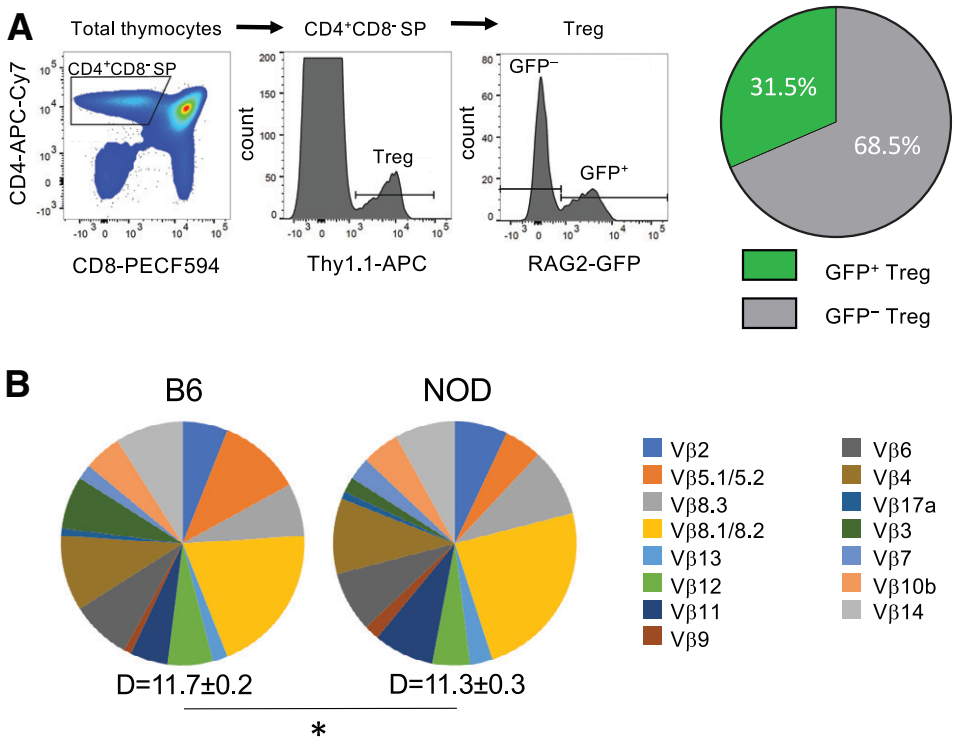

Figure 1—The TCR-Vβ repertoires expressed by Treg newly developed in NOD vs. B6 thymi are similarly diverse. *A*: Thymocytes from 8-week-old *Rag2-Gfp Foxp3-Thy1*^{a} mutant NOD females were analyzed by flow cytometry using antibodies to the indicated markers labeled with indicated fluorochromes. Gating strategy used to sort and quantify newly developed (i.e., GFP^{+}) Treg (left panels). Proportions of newly developed (GFP^{+}) and recirculating (GFP^{-}) cells among thymic Treg (right panels) (n = 14, four independent experiments). *B*: Thymocytes from 8-week-old WT B6 and NOD females were analyzed by flow cytometry using antibodies to CD4, CD8, CD73, CCR7, Foxp3, and a panel of antibodies to indicated TCR-Vβ. Depicted are the mean distributions of TCR-Vβ use among newly developed CD4^{+}CD8^{-}CCR7^{high}CD73$^{-/low}$Foxp3^{+} Treg in indicated mouse strains (see Supplementary Fig. 1 for CCR7/CD73 gates). The indicated diversity measure D is the Shannon diversity (i.e., the exponential of the Shannon entropy, see *Research Designs and Methods* section), represented as mean ± SD (n = 6 mice per strain). *$P < 0.05$ (Mann-Whitney test). In Supplementary Fig. 2*A*, data for individual TCR-Vβ are depicted.

also confirmed the similar diversities of the TRBV repertoires expressed by newly developed NOD and B6 Treg (Fig. 2*B* and Supplementary Table 2). The diversities (i.e., D-values, Shannon diversity) of the TRBV repertoires as determined by TCRseq were higher than those determined by flow cytometry analyses (compared with Fig. 2*B* vs. Fig. 1*B*), because whereas existing antibodies do not cover the entire range of TRBV segments, TCRseq detects all of them. Comparison of the TRBV repertoires as determined by flow cytometry versus TCRseq revealed, as expected, substantial although imperfect similarity (Supplementary Fig. 3). Differences are probably because of the two techniques analyze individual cells and mRNAs, respectively, and each TRBV has its own promoter region, potentially leading to distinct levels of mRNAs in individual cells.

The V-J combination used in a TCR is a critical parameter in its specificity. We therefore assessed the distinct V-J combinations used in TCR expressed by newly developed Treg in NOD and B6 mice. We found some substantial differences in V-J associations used in TCRα and TCRβ expressed by newly developed NOD versus B6 Treg (Supplementary Tables 3 and 4), but the diversities of these associations appeared very large and comparable (Fig. 2*C* and *D*). Rearrangements of the *Tcra* locus continue until positive selection occurs, thus with time, using more upstream V and more downstream J segments (24). To assess the "stringency" of positive selection, we therefore assessed the position-weighted use of V and J segments and found no statistically significant differences between the NOD and B6 *Tcra* sequences (Fig. 2*C* and Supplementary Fig. 4).

The Composition of the CDR3 of TCRs Expressed by Newly Developed NOD and B6 Treg Is Similar

During the course of the distinct thymic selection events, the CDR3s of TCRα and TCRβ chains gradually shorten (34–37). To assess whether newly developed Treg have undergone more or less stringent selection In NOD versus B6 mice, we therefore next used the TCRseq data to assess the CDR3 lengths of the TCRα and TCRβ chains. The average CDR3 lengths of the TCRα and TCRβ chains were identical between NOD and B6 mice (Fig. 2*E* and *F*, left panels). Also the CDR3 length distributions were

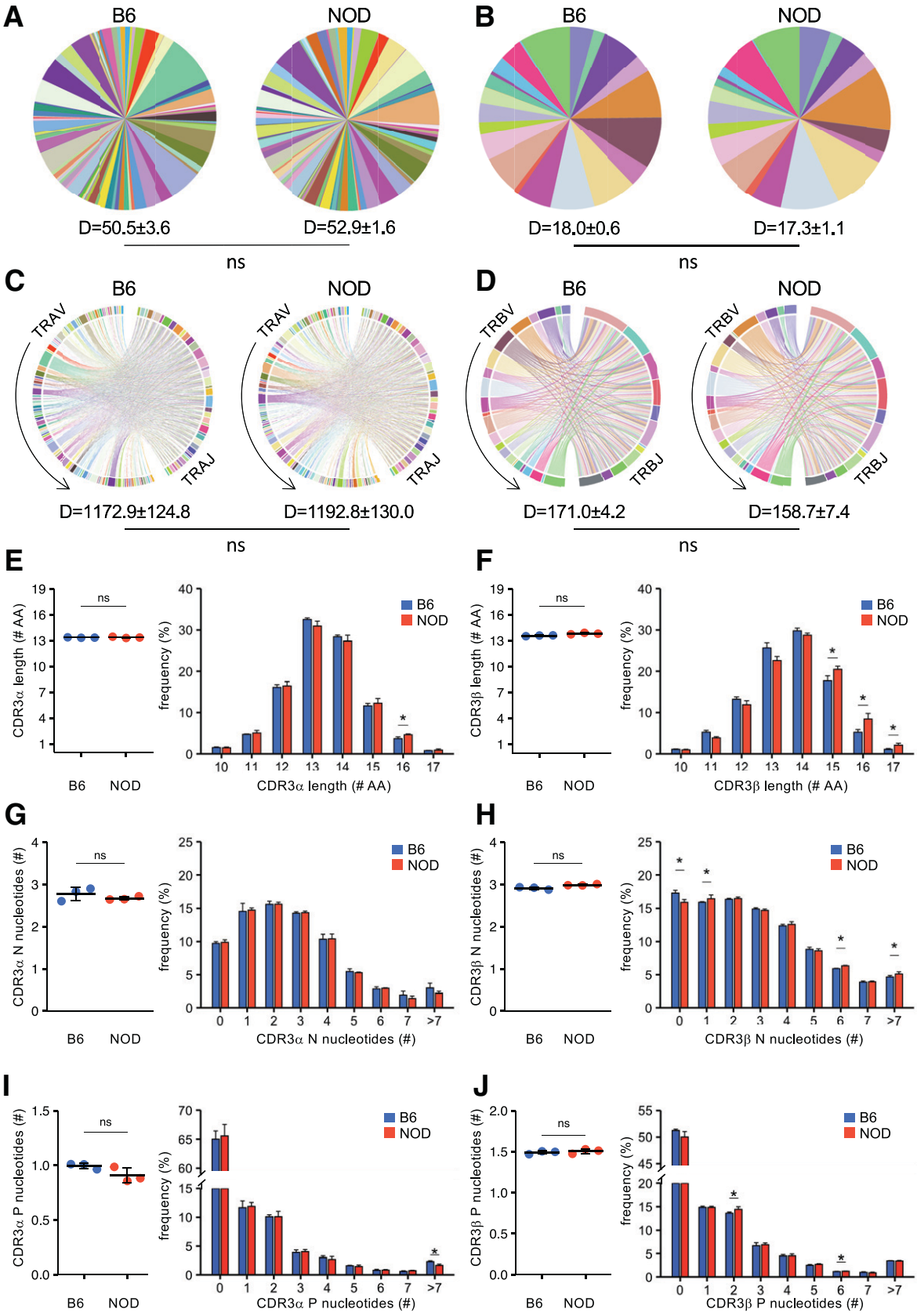

Figure 2—Similar V and J segment use and CDR3 lengths of TCRα and TCRβ expressed by Treg newly developed in NOD vs. B6 thymi $CD4^+CD8^-Thy1.1^+GFP^+$. Treg newly developed in the thymus of 8-week-old *Rag2-Gfp Foxp3-Thy1*^{a} mutant B6 and NOD female mice were sorted by FACS and analyzed by UMI-based TCRseq. TRAV (*A*), TRBV (*B*), TRAV/TRAJ (*C*), and TRBV/TRBJ (*D*) use. Mean values of

practically identical for Treg newly developed in NOD and B6 mice, even if we observed some very small but statistically significant differences (Fig. 2*E* and *F*, right panels).

Non–germline-encoded CDR3 amino acids appear to reduce the affinity of the TCR's interactions with MHC molecules (38). These amino acids are mostly encoded by N and P nucleotides. To assess this parameter, we extracted from the TCRseq data the average numbers and distributions of N and of P nucleotides in the CDR3 regions of the TCRα and TCRβ chains expressed by newly developed Treg. We found that they were practically identical in NOD and B6 mice, even if we observed some very small but statistically significant differences (Fig. 2*G–J*).

The Diversity of TCRα and TCRβ Chains Expressed by Newly Developed NOD and B6 Treg Is Similar

We next assessed the total diversity of the TCRα and TCRβ clonotypes (as characterized by V segment use, CDR3 sequence, and J segment use) expressed by newly developed Treg in NOD and B6 thymi. Rarefaction plots showed similar diversities of TCRα and TCRβ clonotypes expressed by NOD and B6 Treg (Fig. 3*A* and Supplementary Fig. 5*A*). Chao1, Shannon, and Simpson indexes confirmed the similar diversities of TCRα and TCRβ clonotypes in NOD and B6 samples (Fig. 3*B* and Supplementary Fig. 5*B*).

Previous reports indicated that compared with thymic Treg in B6 mice, those in NOD mice expressed a limited diversity of TCRα chains containing TRAV12 and TRAV9 (TRAV2 and TRAV17, respectively, according to the nomenclature of the international ImMunoGeneTics information system, www.imgt.org) (17,18) We therefore also separately analyzed the diversity of TCRα clonotypes using these TRAV. As shown in Fig. 3*C* and *D* and Supplementary Fig. 5*C*, we observed similar diversities in NOD and B6 samples.

The Composition and Diversity of TCRα and TCRβ Chains Expressed by Recirculating Treg in NOD and B6 Thymi Are Similar

These data indicate that the diversities of TCRs expressed by Treg newly developed in the NOD and B6 thymi are similar. This conclusion disagrees, in part, with earlier reports (17,18). One of the several potentially underlying reasons is that, in contrast to the earlier studies, we studied newly developed cells. A difference in the diversities of the very numerous recirculating cells in the pools of Treg in NOD versus B6 thymi (i.e., GFP^- cells in Fig. 1*A*) might provide a partial explanation. To assess this possibility, we performed TCRseq analyses on recirculating $CD4^+CD8^-Thy1.1^+GFP^-$ thymocytes from *Foxp3-Thy1*^{a} *Rag2-Gfp* NOD and B6 mice. Recirculating NOD versus B6 Treg expressed similarly (though not identically) diverse TRAV and TRBV repertoires (Supplementary Fig. 6*A* and *B*) and V-J associations (Supplementary Fig. 6*C* and *D*), and they had similar distributions and average values for CDR3 lengths and numbers of N and P nucleotides (Supplementary Fig. 6*E–J*). They also expressed similarly diverse TCRα and TCRβ repertoires (Supplementary Fig. 7*A* and *B*). Finally, the TRAV2 and TRAV17 repertoires expressed by recirculating Treg were also similarly diverse in NOD versus B6 thymi (Supplementary Fig. 7*C* and *D*).

DISCUSSION

The data we present here indicate that the CDR3 characteristics and the diversities of the TCRα and TCRβ repertoires expressed by Treg newly developed in the thymus of the T1D-prone NOD mouse are very similar to those found in the autoimmune disease-resistant mouse strain B6. This conclusion is principally based on our deep TCRseq analysis of *Tcra*- and *Tcrb*-derived mRNAs that allowed for an unbiased analysis of thousands of cells.

Importantly, TCRseq analysis requires numbers of cells that are very difficult to obtain from single mice. We therefore pooled 8–10 mice per sample analyzed. Whereas pooling several mice would have reinforced the statistical significance of differences found, it eliminates potential interindividual differences that may be biologically significant. It would therefore be of substantial interest to measure the interindividual variation of the diversities and the private and public TCR repertoires expressed by newly developed cells. To address such questions, the TCRseq procedure will need to be further substantially refined.

Despite the generally high levels of similarity, we observed some small differences between the TCR repertoires expressed by Treg newly developed in the thymi of NOD versus B6 mice. Thus, whereas they were similarly diverse, the TRBV and TRAV usages were distinct. This result was most probably due to the different alleles of MHC class II molecules expressed by the two mouse strains, I-A^{g7} for NOD and I-A^b for B6 and, for TRBV, to the distinct MMTV-encoded superantigens encoded in their genomes (39). We also observed some minor but statistically significant differences in CDR3β length distribution between TCRs expressed by newly developing Treg

the three samples are shown. These graphs summarize the data listed in Supplementary Tables 1–4. In *C* and *D*, V and J segments are ordered as in the genome (arrows). Measures of position-dependent use of TRAV and TRAJ are shown in Supplementary Fig. 4. The indicated diversity measure D is the Shannon diversity (i.e., the exponential of the Shannon entropy), represented as mean ± SD. CDR3α (*E*) and CDR3β (*F*) lengths in amino acids (AA). CDR3s starts with conserved Cys and Ala and end with conserved Phe. Number of (non–germline-encoded) N nucleotides (*G* and *H*) and (palindromic) P nucleotides (*I* and *J*) in the CDR3α (*G* and *I*) and CDR3β (*H* and *J*). The left panels in *E–J* indicate mean ± SD, and the right panels indicate distribution (mean ± SD) (n = 3 pools of 8–10 thymi per strain). *$P < 0.05$ by Mann-Whitney test.

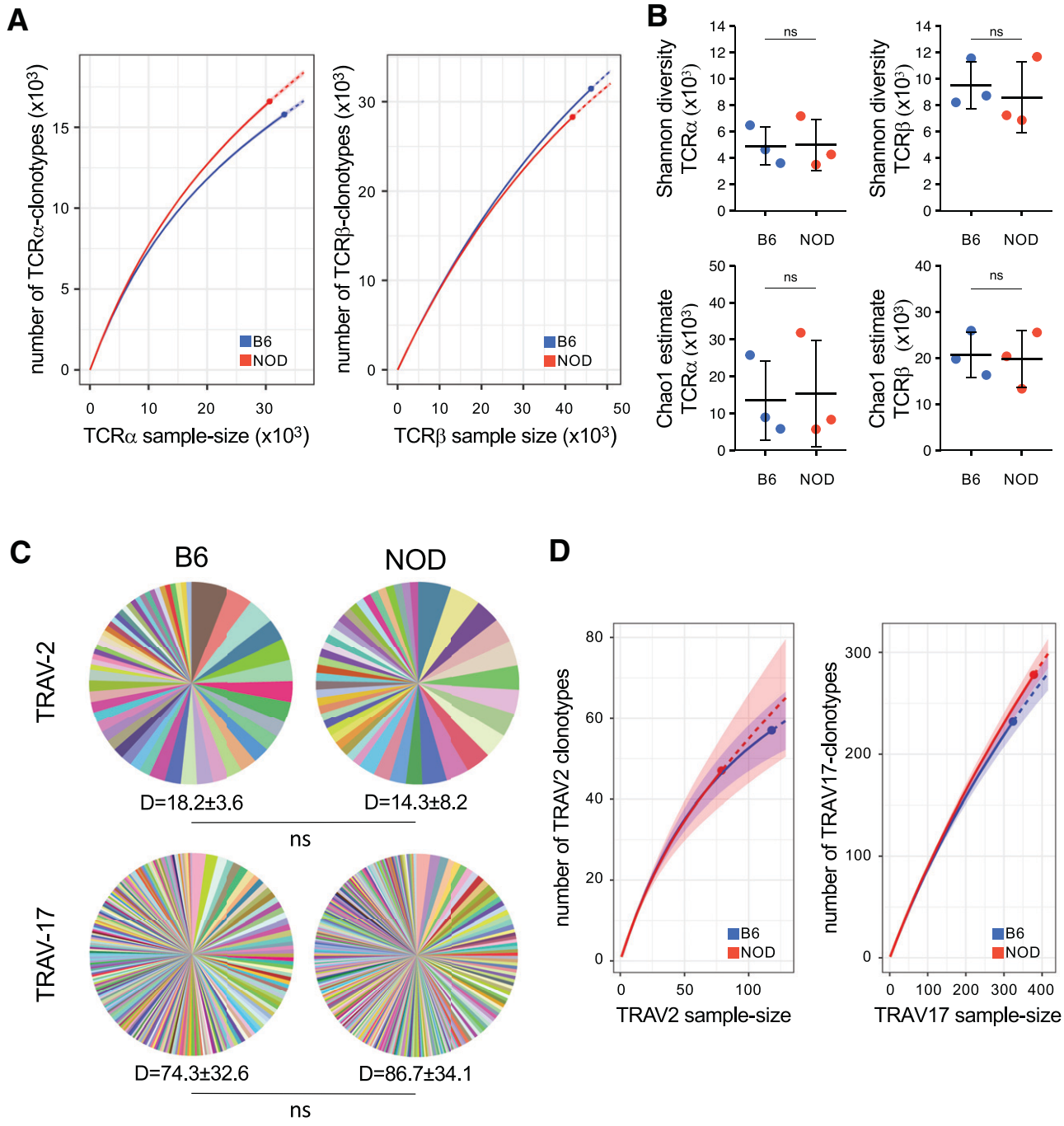

Figure 3—Similar diversities of TCRα and TCRβ clonotypes expressed by Treg newly developed in NOD vs. B6 thymi $CD4^+CD8^-Thy1.1^+GFP^+$. Treg newly developed in the thymi of 8-week-old *Rag2-Gfp Foxp3-Thy1*^{a} mutant B6 and NOD female mice were sorted by FACS and analyzed by UMI-based TCRseq. *A*: Rarefaction plots of data pooled from the three experiments for TCRα (left) and TCRβ (right) clonotypes (as determined by V-use, CDR3 sequence, and J use) in the indicated strains. For rarefaction plots of individual experiments, see Supplementary Fig. 5*A*. Shadows indicate 95% sampling CIs. *B*: Shannon diversities (i.e., the exponential of the Shannon entropy, top) and Chao1 estimates (bottom) for TCRα (left) and TCRβ (right) clonotypes. ns by Mann-Whitney test. Bars indicate mean values ± SD. *C*: Mean clonotype frequencies for TCRα using TRAV2 or TRAV17 in indicated strains. The diversity measure D indicates Shannon diversity ± SD. *D*: Rarefaction plots of pooled data for TCRα using TRAV2 or TRAV17 in indicated strains. Shadows indicate 95% sampling CIs. For rarefaction plots of individual experiments, see Supplementary Fig. 5*C* (n = 3 pools of 8–10 thymi per strain).

in NOD versus B6 mice. Together with some minor differences in the numbers of N and P nucleotides, these observations may again be due to the distinct I-A alleles expressed in NOD versus B6 mice and/or to potentially slightly lower stringencies of the positive and negative selection processes in NOD compared with B6 mice (34–37). Analyses involving MHC-congenic mice will be required to shed light on these different possibilities.

Our results are in part different from previously published data (17,18). In the latter studies, thymic Treg were defined as $CD4^+CD8^-CD25^+$ cells. This population is heterogeneous and contains, besides newly developed Treg, also immature Treg precursors and recirculating Treg (20,40). The recirculating Treg population in the thymus grows steadily with age and is particularly prominent in NOD mice (21). In 5- to 6-week-old NOD and B6 mice, analyzed in the previous reports, this population represents 47 ± 10% and 37 ± 9% of thymic Treg, respectively (21). However, our analysis of the TCR repertoires expressed by recirculating Treg indicated that they were similarly diverse in NOD versus B6 mice, thus excluding this potentially confounding factor. Interestingly, we found that the diversity of the TCR expressed by recirculating Treg in the thymus is very close to that of newly developed cells. Because mainly activated Treg migrate back to the thymus (21), this observation suggests a massive activation of autospecific Treg in the periphery, consistent with previously published data (41). Moreover, approximately half of the previously analyzed $CD4^+CD8^-CD25^+$ cells are $CD25^+Foxp3^-$ Treg precursors (22). Thus, the newly developed Treg population actually represents a small minority of the cells previously analyzed. Using tools that have more recently become available, we were able to sort a pure population of newly developed $Foxp3^+$ Treg. Moreover, the protocol used previously to determine the TCR-Vα encoding sequences was very different from ours. Whereas in the former case TRAV2- and TRAV17-targeted and non–UMI-based amplification of TRAV-cDNAs, followed by cloning and sequencing was used, we used a nonbiased and UMI-based protocol and high-throughput sequencing. The combined differences between the approaches taken previously and in the current study somehow explain the discrepancy of the results. Whatever the precise reason(s), our data indicate that the diversities of the TCRα and TCRβ repertoires expressed by newly developed Treg are very similar in NOD and B6 mice. Also when focusing our analysis on the two TRAVs analyzed previously, we found similar diversities between the repertoires expressed by newly developed NOD versus B6 Treg.

We therefore conclude that the repertoire of TCRs expressed by newly developed Treg in the NOD mouse is of similar diversity as that expressed in the control B6 strain. Importantly, this does not exclude the possibility that essential antigenic specificities may be lacking in the NOD Treg repertoire. Thus, the presentation of tissue-restricted antigens by medullary thymic stromal cells is known to be involved in shaping the TCR repertoire expressed by Treg (15). Genetic differences in expression of tissue-restricted antigens, as previously reported, may, for example, be involved in the susceptibility of the NOD mouse to T1D (42).

Acknowledgments. The authors are very grateful to the following individuals for excellent technical assistance: Fatima L'Faqihi, Valérie Duplan-Eche, Anne-Laure Iscache, Lidia De la Fuente, and Paul Menu of the Center for Pathophysiology of Toulouse Purpan Cytometry Platform, Adrien Castinel and Gwenolah Annonay of the GeT-PlaGE Genotoul, and the personnel of the INSERM US006 Anexplo/Centre Régional d'Exploration Fonctionnelle et Ressources Expérimentales animal facility. The authors are grateful to the members of the "T-cell mediated immune Tolerance team" and to Sylvie Guerder (Center for Pathophysiology of Toulouse Purpan) for discussion and input in the project. J.P.M.v.M. is grateful to the staff of the Biochemistry Institute of the Lausanne University, Epalinges, Switzerland, for its hospitality.

Funding. This work was financially supported by the Fondation pour la Recherche Médicale (FDT201904008280 to J.C.S. and DEQ20160334920 to J.P.M.v.M.), the IdEx Toulouse (to P.R.), the Conseil Régional Midi Pyrénées (15/06/12.05 to J.P.M.v.M.), and the Agence Nationale de la Recherche (ANR-16-CE15-0015-01 to P.R.). A.G.-A., S.C., J.C.S., O.P.J., and J.P.M.v.M. dedicate this work to the memory of their late, much respected, and regretted colleague P.R., who is deceased.

Duality of Interest. No potential conflicts of interest relevant to this article were reported.

Author Contributions. A.G.-A. designed and performed bioinformatic analysis and helped to write the manuscript. S.C. designed and performed experiments and helped to write the manuscript. J.C.S. designed and performed experiments, performed analysis, and helped to write the manuscript. O.P.J. helped in designing the study and analyzing the data and reviewed the manuscript. B.H. analyzed data and helped to write the manuscript. P.R. helped in designing the study and analyzing the data. J.P.M.v.M. designed and supervised the study and wrote the manuscript. J.P.M.v.M. is the guarantor of this work and, as such, had full access to all the data in the study and takes responsibility for the integrity of the data and the accuracy of the data analysis.

References

1. Sakaguchi S, Miyara M, Costantino CM, Hafler DA. FOXP3+ regulatory T cells in the human immune system. Nat Rev Immunol 2010;10:490–500

2. Josefowicz SZ, Lu L-FF, Rudensky AY. Regulatory T cells: mechanisms of differentiation and function. Annu Rev Immunol 2012;30:531–564

3. Panduro M, Benoist C, Mathis D. Tissue tregs. Annu Rev Immunol 2016;34:609–633

4. Bennett CL, Christie J, Ramsdell F, et al. The immune dysregulation, polyendocrinopathy, enteropathy, X-linked syndrome (IPEX) is caused by mutations of FOXP3. Nat Genet 2001;27:20–21

5. Brunkow ME, Jeffery EW, Hjerrild KA, et al. Disruption of a new forkhead/winged-helix protein, scurfin, results in the fatal lymphoproliferative disorder of the scurfy mouse. Nat Genet 2001;27:68–73

6. Long SA, Buckner JH. CD4+FOXP3+ T regulatory cells in human autoimmunity: more than a numbers game. J Immunol 2011;187:2061–2066

7. Romagnoli P, van Meerwijk JPM. Thymic selection and lineage commitment of CD4(+)Foxp3(+) regulatory T lymphocytes. Prog Mol Biol Transl Sci 2010;92:251–277

8. Klein L, Kyewski B, Allen PM, Hogquist KA. Positive and negative selection of the T cell repertoire: what thymocytes see (and don't see). Nat Rev Immunol 2014;14:377–391

9. Romagnoli P, Hudrisier D, van Meerwijk JPM. Preferential recognition of self antigens despite normal thymic deletion of CD4(+)CD25(+) regulatory T cells. J Immunol 2002;168:1644–1648

10. Hsieh CS, Liang Y, Tyznik AJ, Self SG, Liggitt D, Rudensky AY. Recognition of the peripheral self by naturally arising CD25+ CD4+ T cell receptors. Immunity 2004;21:267–277

11. Apert C, Romagnoli P, van Meerwijk JPM. IL-2 and IL-15 dependent thymic development of Foxp3-expressing regulatory T lymphocytes. Protein Cell 2018;9:322–332

12. Tai X, Cowan M, Feigenbaum L, Singer A. CD28 costimulation of developing thymocytes induces Foxp3 expression and regulatory T cell differentiation independently of interleukin 2. Nat Immunol 2005;6:152–162
13. Mahmud SA, Manlove LS, Schmitz HM, et al. Costimulation via the tumor-necrosis factor receptor superfamily couples TCR signal strength to the thymic differentiation of regulatory T cells. Nat Immunol 2014;15:473–481
14. Coquet JM, Ribot JC, Bąbała N, et al. Epithelial and dendritic cells in the thymic medulla promote CD4+Foxp3+ regulatory T cell development via the CD27-CD70 pathway. J Exp Med 2013;210:715–728
15. Yang S, Fujikado N, Kolodin D, Benoist C, Mathis D. Immune tolerance. Regulatory T cells generated early in life play a distinct role in maintaining self-tolerance. Science 2015;348:589–594
16. Salomon B, Lenschow DJ, Rhee L, et al. B7/CD28 costimulation is essential for the homeostasis of the CD4+CD25+ immunoregulatory T cells that control autoimmune diabetes. Immunity 2000;12:431–440
17. Ferreira C, Singh Y, Furmanski AL, Wong FS, Garden OA, Dyson J. Non-obese diabetic mice select a low-diversity repertoire of natural regulatory T cells. Proc Natl Acad Sci U S A 2009;106:8320–8325
18. Ferreira C, Palmer D, Blake K, Garden OA, Dyson J. Reduced regulatory T cell diversity in NOD mice is linked to early events in the thymus. J Immunol 2014;192:4145–4152
19. Wicker LS, Todd JA, Peterson LB. Genetic control of autoimmune diabetes in the NOD mouse. Annu Rev Immunol 1995;13:179–200
20. Thiault N, Darrigues J, Adoue V, et al. Peripheral regulatory T lymphocytes recirculating to the thymus suppress the development of their precursors. Nat Immunol 2015;16:628–634
21. Darrigues J, Santamaria JC, Galindo-Albarrán A, et al. Robust intrathymic development of regulatory T cells in young NOD mice is rapidly restrained by recirculating cells. Eur J Immunol 2021;51:580–593
22. Fontenot JD, Dooley JL, Farr AG, Rudensky AY. Developmental regulation of Foxp3 expression during ontogeny. J Exp Med 2005;202:901–906
23. Yu W, Nagaoka H, Jankovic M, et al. Continued RAG expression in late stages of B cell development and no apparent re-induction after immunization. Nature 1999;400:682–687
24. Borgulya P, Kishi H, Uematsu Y, von Boehmer H. Exclusion and inclusion of alpha and beta T cell receptor alleles. Cell 1992;69:529–537
25. McCaughtry TM, Wilken MS, Hogquist KA. Thymic emigration revisited. J Exp Med 2007;204:2513–2520
26. Romagnoli P, Dooley J, Enault G, et al. The thymic niche does not limit development of the naturally diverse population of mouse regulatory T lymphocytes. J Immunol 2012;189:3831–3837
27. Viret C, Leung-Theung-Long S, Serre L, et al. Thymus-specific serine protease controls autoreactive CD4 T cell development and autoimmune diabetes in mice. J Clin Invest 2011;121:1810–1821
28. Feng Y, van der Veeken J, Shugay M, et al. A mechanism for expansion of regulatory T-cell repertoire and its role in self-tolerance. Nature 2015;528:132–136
29. Britanova OV, Putintseva EV, Shugay M, et al. Age-related decrease in TCR repertoire diversity measured with deep and normalized sequence profiling. J Immunol 2014;192:2689–2698
30. Vander Heiden JA, Yaari G, Uduman M, et al. pRESTO: a toolkit for processing high-throughput sequencing raw reads of lymphocyte receptor repertoires. Bioinformatics 2014;30:1930–1932
31. Bolotin DA, Poslavsky S, Mitrophanov I, et al. MiXCR: software for comprehensive adaptive immunity profiling. Nat Methods 2015;12:380–381
32. Shugay M, Bagaev DV, Turchaninova MA, et al. VDJtools: unifying post-analysis of T cell receptor repertoires. PLoS Comput Biol 2015;11:e1004503
33. Haegeman B, Hamelin J, Moriarty J, Neal P, Dushoff J, Weitz JS. Robust estimation of microbial diversity in theory and in practice. ISME J 2013;7:1092–1101
34. Matsutani T, Ogata M, Fujii Y, et al. Shortening of complementarity determining region 3 of the T cell receptor α chain during thymocyte development. Mol Immunol 2011;48:623–629
35. Yassai M, Gorski J. Thymocyte maturation: selection for in-frame TCR α-chain rearrangement is followed by selection for shorter TCR β-chain complementarity-determining region 3. J Immunol 2000;165:3706–3712
36. Yassai M, Ammon K, Goverman J, Marrack P, Naumov Y, Gorski J. A molecular marker for thymocyte-positive selection: selection of CD4 single-positive thymocytes with shorter TCRB CDR3 during T cell development. J Immunol 2002;168:3801–3807
37. Matsutani T, Ohmori T, Ogata M, et al. Comparison of CDR3 length among thymocyte subpopulations: impacts of MHC and BV segment on the CDR3 shortening. Mol Immunol 2007;44:2378–2387
38. Gilfillan S, Waltzinger C, Benoist C, Mathis D. More efficient positive selection of thymocytes in mice lacking terminal deoxynucleotidyl transferase. Int Immunol 1994;6:1681–1686
39. Luther SA, Acha-Orbea H. Mouse mammary tumor virus: immunological interplays between virus and host. Adv Immunol 1997;65:139–243
40. Lio CWJ, Hsieh CS. A two-step process for thymic regulatory T cell development. Immunity 2008;28:100–111
41. Fisson S, Darrasse-Jèze G, Litvinova E, et al. Continuous activation of autoreactive CD4+ CD25+ regulatory T cells in the steady state. J Exp Med 2003;198:737–746
42. Venanzi ES, Melamed R, Mathis D, Benoist C. The variable immunological self: genetic variation and nongenetic noise in Aire-regulated transcription. Proc Natl Acad Sci U S A 2008;105:15860–15865